INVESTIGATIONS OF LIQUID PHASE TURBULENCE BASED ON DIRECT NUMERICAL SIMULATIONS OF BUBBLY FLOWS

Milica Ilić
Institute for Reactor Safety, Forschungszentrum Karlsruhe, Postfach 3640, 76021 Karlsruhe, Germany
Phone: +49 (0) 72 47 82 29 49, Fax: +49 (0) 72 47 82 37 18, E-Mail: ilic@irs.fzk.de

Martin Wörner[1]
Institute for Reactor Safety, Forschungszentrum Karlsruhe, Postfach 3640, 76021 Karlsruhe, Germany
Phone: +49 (0) 72 47 82 25 77, Fax: +49 (0) 72 47 82 37 18, E-Mail: woerner@irs.fzk.de

Dan G. Cacuci
Institute for Nuclear Technology and Reactor Safety, University of Karlsruhe, Haid und Neu Str. 7, 76131 Karlsruhe, Germany
Phone: +49 (0) 72 16 08 67 40, Fax: +49 (0) 72 16 08 67 49, cacuci@ikr.uni-karlsruhe.de

ABSTRACT

This paper presents investigations of liquid velocity fluctuations based on direct numerical simulations of bubbly flows. Investigations are performed by statistical analysis of instantaneous liquid flows generated by rise of monodisperse bubble swarms through initially quiescent liquid within a plane channel. Effects of bubble rise velocity, bubble trajectory and bubble shape are analyzed considering gas-liquid suspensions with different viscosity. The ultimate goal of the performed research was to shed some light on mechanisms governing behaviour of liquid turbulence kinetic energy in bubble-driven liquid flows. In relation to this quantitative analysis of the basic balance equation for liquid turbulence kinetic energy is performed and the obtained results are used to assess performance of corresponding closure assumptions applied in engineering turbulence models. Evaluations based on rigorous mathematical formulations revealed that the fluctuating liquid flow is supplied with energy only through the work of fluctuating liquid stress upon moving bubble interfaces. As this mechanism is related to the presence of bubbles, the local non-equilibrium between the turbulence generation and turbulence dissipation results in an intensive diffusion transport of liquid turbulence kinetic energy from the domains of high gas volumetric fractions to the regions with low gas contents. All currently used engineering formulations overestimate the production term and underestimate the diffusion term. The dissipation term modelling in one-equation models is, also, inaccurate. On the other hand, the approximation of the interfacial turbulence generation by the rate of the work of the drag force performs quite well.

KEYWORDS

bubbly flows, direct numerical simulations, bubble-induced turbulence, liquid turbulence kinetic energy

1 INTRODUCTION

Bubbly gas-liquid flows are widely used in engineering systems such as power generation, chemical engineering and metallurgical facilities. The flow regimes applied in these systems span from very slow buoyancy driven flows in bubble-columns and air-lift rectors to forced flows in pipes and ducts. Whatever the regime under consideration, low or high Reynolds number, all bubbly flows have a common characteristic - the relative motion of bubbles induces fluctuations of liquid phase quantities. These fluctuations are caused not only by non-linearity of the flow, but also by the discrete buoyancy distribution, motion of wakes behind bubbles and deformation of bubble interfaces. Such perturbations

[1]Corresponding author

of the liquid phase give rise to Reynolds stresses and other phenomena inherent to turbulence. Consequently, the phenomenon is named *bubble-induced turbulence*.

Examples of bubble-induced turbulence are encountered in various industrial processes involving slow very dispersed gas-liquid flows where no shear-induced turbulence occurs and where the main flow features such as distribution of phases and mixing are controlled only by agitation of the liquid phase by moving bubbles. A realistic description of the bubble-induced turbulence is, therefore, one of the most fundamental requests for an accurate modelling of such bubbly flows.

Among several engineering approaches commonly used to predict the bubble-induced turbulence far the most popular concept is based on *the balance equation for turbulence kinetic energy of the liquid phase* (hereafter called k_l equation). Balance terms in this equation are formulated by an extension of corresponding closure assumptions well-established for single-phase flows, while the effects of suspended bubble interfaces are either completely ignored or implemented through more or less empirically derived model terms. As it is not clear whether / how far closure assumptions originally developed for single-phase flows can retain their validity when the dispersed phase is present, such an approach might be argued as highly uncertain. Further, proposed closure relations for interfacial turbulence effects differ from author to author conspicuously with model parameters mainly fitted to the particular problem under consideration.

Most of the difficulties faced in the development of improved closure assumptions for balance terms in k_l equation concern an extremely poor understanding of mechanisms in which bubbles alter turbulence generation, redistribution and dissipation in the liquid phase. Mathematically, these mechanisms were rigorously formulated by the basic balance equation for the liquid turbulence kinetic energy in gas-liquid flows (Kataoka & Serizawa, 1989). However, although known for more than a decade this equation could not be exposed to an appropriate quantitative analysis, because highly resolved data about the flow field and phase interface structure have not been available.

Recent improvements in computer performances and positive experience from single-phase flows suggest use of *direct numerical simulations* (DNS). Although associated with serious limitations concerning the magnitude of liquid Reynolds number and the number of bubbles that can be tracked, DNS open a new promising way to gain a detailed insight into mechanisms governing the liquid phase turbulence in the aforementioned slow dilute bubbly flows. Among these, the simplest case concerns a confined multi-phase flow where gas phase is through a distributor sparged into a quiescent liquid medium. A prominent example of such a flow is encountered in flat bubble columns widely used as multi-phase contactors and reactors in chemical and metallurgical industries.

Current DNS based liquid turbulence analyzes employ the concept of fully periodic computational domain where an unbounded steady bubbly flow with uniformly sized bubbles and no bubble coalescence is approximated by infinite arrays of identical monodisperse bubble-swarms (Bunner & Tryggvason, 2003). In this way a homogeneous bubbly flow, that allows the use of volume averaging, is put into consideration. This flow configuration is, however, not appropriate for a quantitative analysis of k_l equation because the imposed spatial uniformity excludes the considerations of the diffusion transport as well as the energy transfer between the mean and fluctuating liquid flow. Consequently, the reported turbulence investigations are restricted to evaluations of the liquid turbulence kinetic energy and its dissipation rate.

At the Institute for Reactor Safety in the Research Centre Karlsruhe *the computer code TURBIT-VoF* for direct numerical simulations of incompressible gas-liquid flows has been developed (Sabisch *et al.* , 2001). Different to other DNS codes, TURBIT-VoF is designed to perform computations of bubbly flows within a domain bounded with two rigid walls. DNS of multiple bubble systems by TURBIT-VoF can, therefore, quite realistically approximate a non-homogeneous developed gas-liquid flow within a flat bubble column with a moderate ratio of the bubble diameter to the column depth and, in this

way, provide an appropriate input data basis for the corresponding analysis of mechanisms governing behaviour of liquid turbulence kinetic energy.

In the context of the aforementioned, this paper reports DNS based investigations of liquid velocity fluctuations generated by rise of monodisperse bubble-swarms within a plane infinite channel. In particular, the effects of different bubble rise velocity, bubble trajectory and bubble shape on generated fluctuating liquid flow are investigated by considering three gas-liquid suspensions with different viscosity.

The paper is organized as follows. In Section 2 the applied methodology and specified computational set-up for DNS of bubbly flows by TURBIT-VoF are outlined. Section 3 deals with computed bubble dynamics and characteristics of the generated liquid phase flow with a special attention paid to the distribution of liquid turbulence kinetic energy. Section 4 focuses on the quantitative analysis of balance equation for liquid turbulence kinetic energy. Results for diffusion transport, viscous dissipation, interfacial generation and transfer of energy between the mean and fluctuating liquid flow evaluated by their basic definitions are in Section 5 used to test performance of corresponding closure assumptions commonly used in engineering turbulence models. The paper is completed by conclusions.

2 DIRECT NUMERICAL SIMULATIONS OF BUBBLY FLOWS BY COMPUTER CODE TURBIT-VoF

2.1 Methodology of TURBIT-VoF

An incompressible flow of two immiscible Newtonian fluids is in TURBIT-VoF described by a single set of balance equations for mass (equation 1) and momentum (equation 2):

$$\mathrm{div}\mathbf{U} = 0 \quad \text{and} \tag{1}$$

$$\frac{\partial \rho \mathbf{U}}{\partial \theta} + \mathrm{div}(\rho \mathbf{U}\mathbf{U}) = -\mathrm{grad}P + \frac{1}{\mathrm{Re}_{ref}}\mathrm{div}\mathbf{T} - \frac{(1-f-\langle\alpha_g\rangle)\mathrm{E\ddot{o}}_{ref}}{\mathrm{We}_{ref}}\frac{\mathbf{g}}{|\mathbf{g}|} + \frac{\kappa A_{in}}{\mathrm{We}_{ref}}\mathbf{n}, \tag{2}$$

while the flow regions containing pure liquid are distinguished from the pure gas ones employing the transport equation for the liquid volumetric fraction:

$$\frac{\partial f}{\partial \theta} + \mathrm{div}(\mathbf{U}f) = 0. \tag{3}$$

The equations 1 - 3 are given in dimensionless form. The following scaling applies: distance, $\mathbf{X} = \mathbf{x}/l_{ref}$, velocity, $\mathbf{U} = \mathbf{u}/u_{ref}$, time, $\theta = \vartheta u_{ref}/l_{ref}$ and density, $\rho = \varrho/\varrho_{ref}$, where material properties of the liquid phase, density and viscosity, are taken to be reference values ($\varrho_{ref} = \varrho_l$ and $\mu_{ref} = \mu_l$), whereas the reference length, l_{ref}, and the reference velocity, u_{ref}, are to be specified. Reference Reynolds number, reference Weber number and reference Eötvös number are, respectively, defined as: $\mathrm{Re}_{ref} = \varrho_l u_{ref} l_{ref}/\mu_l$, $\mathrm{We}_{ref} = \varrho_l u_{ref}^2 l_{ref}/\sigma$, and $\mathrm{E\ddot{o}}_{ref} = (\varrho_l - \varrho_g)|\mathbf{g}|l_{ref}^2/\sigma$, where σ stands for the surface tension and $\mathbf{g}$ represents the gravity, while subscripts l and g denote the liquid and the gas phase, respectively.

In order to prevent a uniform downward acceleration of the whole system and to ensure by the same time a downward liquid flow in the vicinity of channel walls, an additional body force, $\langle\varrho\rangle\mathbf{g}$, is imposed to both fluids, where $\langle\varrho\rangle = \varrho_l + \langle\alpha_g\rangle(\varrho_g - \varrho_l)$ represents the overall density of two-phase mixture. In relation to this, the dimensionless pressure is defined as $P = (p - \varrho_l \mathbf{g}\cdot\mathbf{x})/(\varrho_l u_{ref}^2)$, while the buoyancy term involves the overall gas volumetric fraction, $\langle\alpha_g\rangle$. The contribution of the surface tension force is expressed by the last term in the momentum equation, where κ stands for twice the mean interface curvature, $\mathbf{n}$ indicates the unit normal vector to the phase interface pointing from the gas into the liquid

and A_{in} represents the dimensionless interfacial area concentration.

A computational cell is filled with the liquid phase when $f = 1$ or with the gas when $f = 0$. If $0 < f < 1$, an interface exists within the cell. In such cells the model of a homogeneous two-phase mixture is applied where the equality of phase velocities and pressures is assumed and where the mixture density and viscosity are expressed as: $\varrho = f\varrho_l + (1-f)\varrho_g$ and $\mu = f\mu_l + (1-f)\mu_g$.

The equation 3 is numerically solved employing a Volume-of-Fluid (VoF) procedure. First, the interface orientation and location inside each mesh cell is reconstructed using PLIC (*P*iecewise *L*inear *I*nterface *C*alculation) method EPIRA which locally approximates interface by a plane. In the second step, the liquid fluxes across the faces of the mesh cell are computed and the interface is advected. The methodology is verified comparing numerical results with experimental data for the rise of an ellipsoidal bubble and an oblate ellipsoidal cap bubble (Sabisch *et al.* , 2001).

2.2 Computational Setup for Direct Numerical Simulations of Bubbly Flows by TURBIT-VoF

Employing TURBIT-VoF three numerical experiments are performed where the motion of monodisperse swarms consisting of 8 bubbles within a plane channel bounded with two rigid walls is simulated.

The following parameters are common for all the simulations. The computational domain is specified to be a cube of the size $l = l_{ref}$ and discretized with 64^3 uniform mesh cells. The equivalent bubble diameter, d_b, is prescribed to be one fourth of the computational domain size what results in the overall gas volumetric fraction $\langle\alpha_g\rangle = 6.544\%$. The ratios of phase densities and phase viscosities are, respectively, specified as $\varrho_g/\varrho_l = 0.5$ and $\mu_g/\mu_l = 1$. Bubble Eötvös number is adopted to be $E\ddot{o}_b = 3.065$.

In order to analyze the effects of different bubble rise velocity, different bubble shape and different bubble trajectories, values of specified Morton number differ by two orders of magnitude. A preliminary estimation based on the diagram of Clift *et al.* (1978) shows, namely, that a bubbly flow with spherical bubbles is expected when $M = 3.06 \cdot 10^{-2}$ (further called scenario 8BM2), with slightly ellipsoidal bubbles when $M = 3.06 \cdot 10^{-4}$ (scenario 8BM4) and with ellipsoidal bubbles when $M = 3.06 \cdot 10^{-6}$ (scenario 8BM6). Physically, such a decrease of Morton number while keeping bubble Eötvös number constant can be achieved by choosing the liquid of a lower viscosity. In relation to this, corresponding liquid viscosities relative to the viscosity in the scenario 8BM2 stand in the following ratio:

$$\mu_{l,r}^{8\mathrm{BM6}} : \mu_{l,r}^{8\mathrm{BM4}} : \mu_{l,r}^{8\mathrm{BM2}} = 0.1 : 0.316 : 1, \tag{4}$$

where the superscripts indicate simulation scenarios and the subscript r indicates the division with $\mu_l^{8\mathrm{BM2}}$.

3 STATISTICAL ANALYSIS OF COMPUTED BUBBLY FLOWS

3.1 Three-dimensional Bubble Motion and Instantaneous Liquid Flow

The visualization of the bubble shape and liquid phase velocities in representative wall-normal planes for simulated bubbly flow scenarios is presented in Figure 1, while the main DNS results concerning the dynamics of bubbles are summarized in Table 1.

In the most viscous case 8BM2 no bubble deformation is observed, i.e. bubbles retained their initial spherical shape. The evaluation of bubble trajectories has shown that individual bubbles move almost rectilinearly keeping initially prescribed distances from each other. A detailed inspection of the liquid flow structure revealed no existence of bubble wakes, what leads to the conclusion that the generated liquid motion is the result of pure liquid displacement by moving bubbles. A rather different flow configuration is seen in Figure 1c - only slightly ellipsoidal bubbles in scenario 8BM4 agitate the liquid

Simulation scenario	low viscosity 8BM6	medium viscosity 8BM4	high viscosity 8BM2
computed time [a]	3	2.15	2.1
computed rise length [a]	6.89	2.26	0.94
lateral bubble motion[c]	strong	slight	negligible
mean bubble rise velocity [ab]	2.38	1.25	0.46
mean bubble axis aspect ratio [b]	1.526	1.132	1

[a] dimensionless
[b] in steady state
[c] during the whole simulation period

Table 1: List of main DNS results for the dynamics of simulated bubbly flows.

phase considerably, not only through the liquid displacement, but also through the formation of vortical structures. Comparing to the case 8BM2 larger lateral deviations of individual bubble trajectories can be observed in Figure 1d. In the low viscous case 8BM6 bubbles are oblate ellipsoids moving along non-rectilinear paths with pronounced lateral deviations (see Figure 1f). Although displayed only in one wall-normal section, perturbations of the liquid phase velocity are evident, not only due to the bubble-induced liquid displacement, but, also, due to the formation and mutual interaction of bubble wakes (see Figure 1e).

Finally, the following is stressed. In all the presented simulations of bubbly flows by TURBIT-VoF a steady flow regime has been reached and kept sufficiently long to provide a complete data basis for the statistical analysis of bubble-induced velocity fluctuations of the liquid phase.

3.2 Averaging of Instantaneous Liquid Flow

A statistical analysis of bubble-induced liquid motion based on time averaging requires the knowledge of the instantaneous liquid flow for each computed time instant and over the whole computational domain. A storage of such an amount of DNS data requires, however, a huge memory space. For instance, in the statistical analysis of liquid fluctuations for the bubbly flow scenario 8BM6 the steady state regime within the time interval $\theta = 0.6 - 2.5$ should be considered. With the specified time step width $\Delta\theta = 0.5 \cdot 10^{-4}$ this means that 38000 full data sets would have to be stored.

Fortunately, the configuration of the considered bubbly flows offers a possibility for an application of a spatial averaging that is associated with significantly lower memory requests. When one, namely, takes into account that all the analysis concern the steady developed flow regime where the liquid flow within a doubly periodic domain is driven by two distinctive densely packed bubble populations rising approximatively parallel to the channel walls, it might be assumed that perturbations of the liquid phase spatially depend only on the wall-normal coordinate, x_3. This implies that the liquid turbulence structure in both, the vertical and the span-wise, directions might be considered as homogeneous, what further allows the averaging over vertical slabs of mesh cells parallel to the channel walls.

In the context of aforementioned, the averaging performed here is defined as:

$$\overline{A}_\gamma = \frac{1}{m_1 m_2} \sum_{\alpha=1}^{m_1} \sum_{\beta=1}^{m_2} A_{\alpha\beta\gamma}, \tag{5}$$

where subscripts α, β and γ denote Cartesian coordinate directions and m_1 and m_2 represent, respectively, the number of mesh cells in the vertical and span-wise direction. Since the concept of DNS assumes that the liquid phase indicator function may be replaced by the local liquid volumetric fraction, f, mean

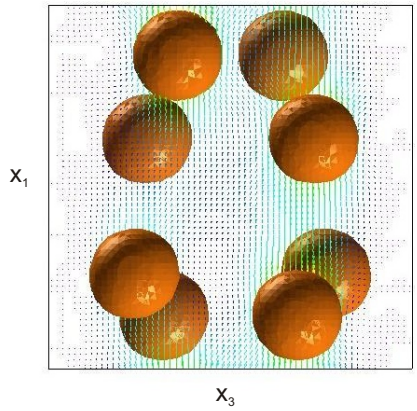

(a) scenario 8BM2 ($x_2 = 0.734$)

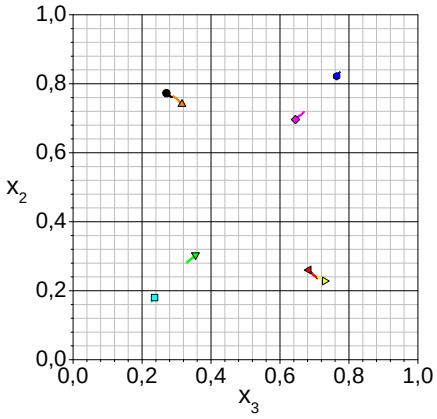

(b)

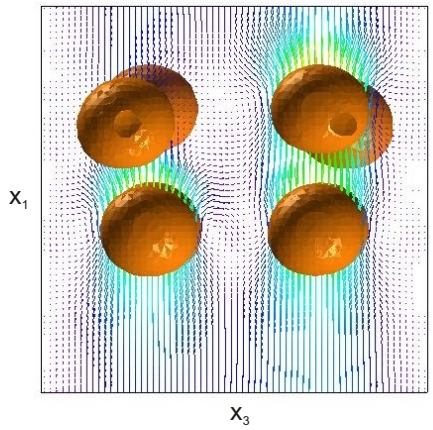

(c) scenario 8BM4 ($x_2 = 0.734$)

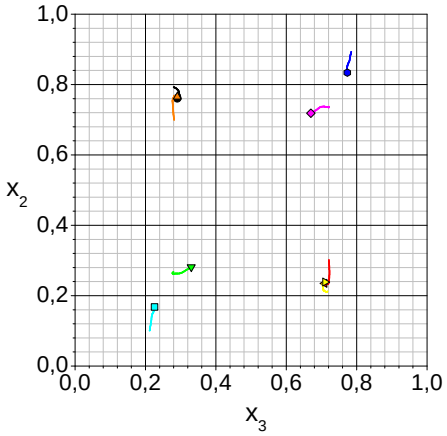

(d)

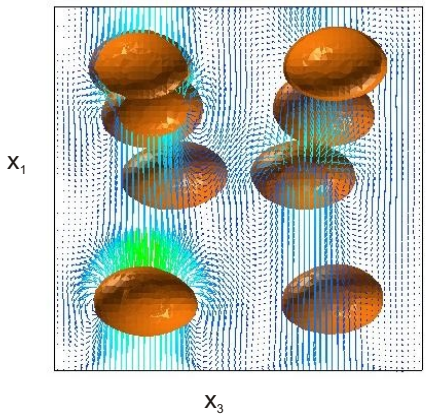

(e) scenario 8BM6 ($x_2 = 0.781$)

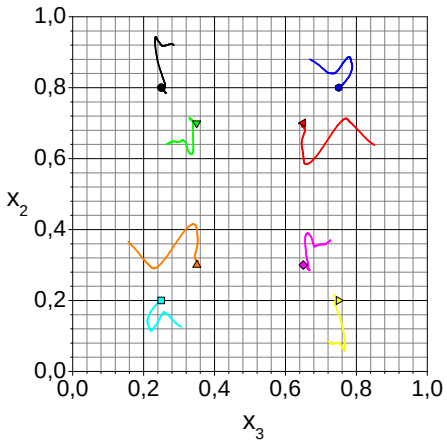

(f)

Figure 1: Visualization of computed bubbly flows: left - bubble shape and liquid velocities at representative span-wise positions, x_2, right - lateral bubble movements (symbols represent initial bubble positions).

magnitudes of the liquid and gas volumetric fraction are, respectively, computed as:

$$\alpha_{l\gamma} = \frac{1}{m_1 m_2} \sum_{\alpha=1}^{m_1} \sum_{\beta=1}^{m_2} f_{\alpha\beta\gamma} \quad \text{and} \quad \alpha_{g\gamma} = \frac{1}{m_1 m_2} \sum_{\alpha=1}^{m_1} \sum_{\beta=1}^{m_2} (1 - f_{\alpha\beta\gamma}), \tag{6}$$

while phase-weighted liquid quantities are evaluated from:

$$\overline{\overline{A}}_{l\gamma} = \frac{1}{\alpha_{l\gamma}} \frac{1}{m_1 m_2} \sum_{\alpha=1}^{m_1} \sum_{\beta=1}^{m_2} f_{\alpha\beta\gamma} A_{\alpha\beta\gamma}. \tag{7}$$

Liquid phase fluctuations in the bulk fluid and at the liquid side of phase interface are, respectively, computed from:

$$A'_{l\alpha\beta\gamma} = A_{l\alpha\beta\gamma} - \overline{\overline{A}}_{l\gamma} \quad \text{and} \quad A'_{li\alpha\beta\gamma} = A_{li\alpha\beta\gamma} - \overline{\overline{A}}_{l\gamma}, \tag{8}$$

where the subscript i indicates an interfacial liquid quantity.

The presented averaging technique can successfully be performed using DNS data for any single time instant within the steady regime of a considered bubbly flow. However, in order to obtain smooth profiles of liquid turbulence quantities the following procedure is applied. First, evaluations based on spatial averaging are done for the number of time steps within the interval of fully developed flow regime and then the arithmetic mean of the results obtained for individual time instances is computed.

3.3 Distribution of Liquid Turbulence Kinetic Energy

Due to its relevance to the topic considered in this paper the attention in this section is focused on the distribution of liquid turbulence kinetic energy in simulated bubbly flows.

Wall-normal profiles of liquid turbulence kinetic energy,

$$k_l = \frac{1}{2} \overline{\overline{\mathbf{u}'_l \cdot \mathbf{u}'_l}}, \tag{9}$$

are presented in Figure 2 for different bubbly flow scenarios. Figure 2 shows that k_l drastically decreases with the increase of the liquid viscosity. The evaluation of the overall liquid turbulence kinetic energy, $\langle k_l \rangle$, has revealed a non-linear nature of the dependance $\langle k_l \rangle = f(\mu_l)$: in the range of less viscous flows (scenario 8BM6 to 8BM4) the increase of the liquid viscosity of 3.162 times decreases $\langle k_l \rangle$ by the factor of 4.233, whereas for more viscous flows (scenario 8BM2 to 8BM4) the same increase of the liquid viscosity results in 9.812 times lower values of $\langle k_l \rangle$. Taking into account the differences of the considered flow configurations, at least three parameters associated with such a behaviour of the liquid turbulence kinetic energy can be identified: the magnitude of the bubble velocity, the bubble shape (reflected through added mass) and the formation of bubble wakes.

The bubble rise velocity, $\langle u_b \rangle$, certainly strongly influences magnitudes of the liquid turbulence kinetic energy in here considered bubbly flows since $\langle u_b \rangle$ dramatically decreases with the increase of the liquid viscosity (see Table 1). However, a rough estimate shows that the dependance $\langle k_l \rangle = f(\mu_l)$ is remarkably steeper than the dependance $\langle u_b \rangle^2 = g(\mu_l)$, what gives rise to the consideration of effects related to the added mass.

The added mass for a bubble with volume V_b and axis aspect ratio χ is defined as (Wijngaarden, 1998):

$$m_{am} = Q(\kappa) \frac{1}{2} \varrho_l V_b, \tag{10}$$

where:

$$Q(\chi) = 2 \frac{(\chi^2 - 1)^{1/2} - \cos^{-1} \chi^{-1}}{\cos^{-1} \chi^{-1} - (\chi^2 - 1)^{1/2} / \chi^2}. \tag{11}$$

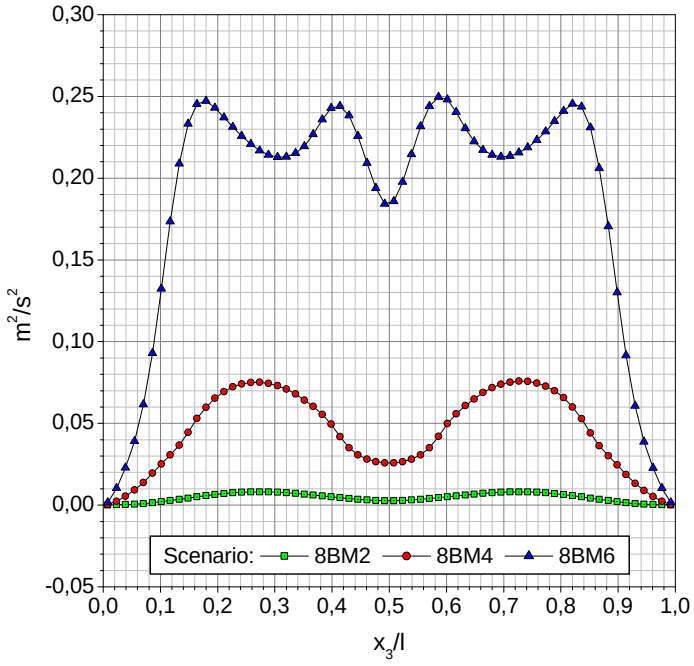

Figure 2: Kinetic energy of liquid velocity fluctuations generated by bubble rise through liquids with different viscosity.

Using the above relations and the data on bubble axis aspect ratio from Table 1 it can be shown that compared to the bubbly flow case with spherical bubbles (scenario 8BM2) the magnitude of liquid turbulence kinetic energy should be higher 1.159 times in the case 8BM4 and even 1.641 times in the case 8BM6 only due to the ellipsoidal bubble shape in the two latter scenarios.

Finally, effects of bubble wakes on the distribution of liquid turbulence kinetic energy can be observed analyzing the shapes of corresponding k_l profiles given in Figure 2. Therefore, while k_l profiles in the cases 8BM2 and 8BM4, where the influence of bubble wakes is very weak, are smooth, k_l profile in the case 8BM6 has a double saddle-like shape with pronounced peaks in the domains of low gas volumetric fractions. The analysis of the instantaneous liquid velocity field has shown that these peaks are caused by the formation of intensive vortical structures around the bubble equator.

An attempt to elucidate mechanisms governing the aforementioned complex behaviour of liquid turbulence kinetic energy in slow bubble-driven liquid flows is presented in the next section.

4 QUANTITATIVE ANALYSIS OF BALANCE EQUATION FOR LIQUID TURBULENCE KINETIC ENERGY IN SIMULATED BUBBLY FLOWS

Based on local instant and averaged formulations of mass and momentum conservation laws for gas-liquid flows Kataoka & Serizawa (1989) derived balance equation for turbulence kinetic energy of consisting phases. When the liquid phase is considered, this equation takes the following form:

$$\underbrace{\frac{\partial}{\partial\vartheta}(\alpha_l k_l)}_{\text{unsteady term}} + \underbrace{\frac{\partial}{\partial x_\beta}(\alpha_l k_l \bar{\bar{u}}_{l\beta})}_{\text{convective term}} = \underbrace{-\frac{\partial}{\partial x_\alpha}(\alpha_l \overline{\overline{p'_l u'_{l\alpha}}}) - \frac{\partial}{\partial x_\beta}(\alpha_l \frac{1}{2}\overline{\overline{u'_{l\alpha} u'_{l\alpha} u'_{l\beta}}}) + \frac{\partial}{\partial x_\beta}(\alpha_l \overline{\overline{\tau'_{l\alpha\beta} u'_{l\alpha}}})}_{\text{diffusion, Diff}(k_l)}$$

$$\underbrace{-\alpha_l \overline{\overline{\tau'_{l\alpha\beta}}} \frac{\partial u'_{l\alpha}}{\partial x_\beta}}_{\text{dissipation, } \varepsilon_l} \underbrace{-\alpha_l \overline{\overline{u'_{l\alpha} u'_{l\beta}}} \frac{\partial \bar{\bar{u}}_{l\alpha}}{\partial x_\beta}}_{\text{production, } \Pi_l} \underbrace{-\overline{p'_{li} u'_{li\alpha}} n_{l\alpha} a_i + \overline{\tau'_{li\alpha\beta} u'_{li\alpha}} n_{l\beta} a_i}_{\text{interfacial terms, } \Upsilon_l}, \qquad (12)$$

where Einstein's summation rule applies to α and β and does not apply to l, g and i. An evaluation of balance terms in equation 12 offers a possibility for the analysis of mechanisms in which bubbles alter the liquid turbulence generation, dissipation and redistribution as well as its interplay with flow parameters such as velocity field, phase distribution and interfacial structures. The evaluations presented here comprise balance terms on the right-hand-side of the equation 12. Due to the adopted averaging technique, namely, magnitudes of the convective term can be neglected. Further, since only steady flow regimes are considered the unsteady term is, also, negligible.

The budget of the basic balance equation for the turbulence kinetic energy of the liquid phase presented in Figure 3 revealed the prominent role of the interfacial terms. Since magnitudes of the production term are, namely, so low that it can be neglected, the generation of liquid turbulence kinetic energy is continuously maintained by moving bubbles through the work of fluctuating liquid stress upon the bubble interfaces. However, as the interfacial generation of liquid turbulence kinetic energy is strictly related to the bubble presence, profiles of interfacial terms consist of parabolic-like pieces with high values in domains of high gas volumetric fractions and zero values in regions permanently occupied by the liquid phase. On the other side, although the dissipation rate of liquid turbulence kinetic energy in two-phase regions is remarkably more intensive than in single-phase parts, the dissipation profiles are non-zero valued along the whole channel width. The local balance can, therefore, be established only if some energy from the two-phase domains is transported towards the single-phase regions. Indeed, Figure 3 shows that the significant portion of the liquid turbulence kinetic energy produced by moving bubble interfaces diffuses towards the parts of the channel occupied only by the liquid phase.

5 ASSESSMENT OF CLOSURE ASSUMPTIONS FOR BALANCE TERMS IN TURBULENCE KINETIC ENERGY EQUATION OF LIQUID PHASE

Since the results presented in the previous section are obtained on the basis of rigorous mathematical formulations for balance terms given by equation 12, they may be considered as exact, and, in this context, used to test the assessment of corresponding closure assumptions commonly applied in engineering liquid turbulence models (further called modelled terms). In this section more detailed considerations of individual balance terms in equation 12 are presented from that point of view.

5.1 Transfer of Kinetic Energy Between Mean and Fluctuating Liquid Flow

The transfer of kinetic energy between the mean and fluctuating flow is called production, because in shear flows it is always the source of turbulence kinetic energy. Predictions of the production term in engineering liquid turbulence models for bubbly flows are based on the following single-phase-like closure assumption:

$$\Pi_l = \alpha_l \nu_l^{\text{eff}} [\nabla \overline{\overline{\mathbf{u}}}_l + \nabla \overline{\overline{\mathbf{u}}}_l^T] : \nabla \overline{\overline{\mathbf{u}}}_l \tag{13}$$

where ν_l^{eff} represents the effective viscosity of the liquid phase.

In one-equation ($k-l$) models the liquid effective viscosity, ν_l^{eff}, is given by (Kataoka & Serizawa, 1995a), (Kataoka & Serizawa, 1995b):

$$\nu_l^{\text{eff}} = \beta_1 l_{tp} \sqrt{k_l}, \tag{14}$$

where l_{tp} denotes the two-phase mixing length and the coefficient $\beta_1 = 0.56$. It is noted that, the method proposed for the determination of l_{tp} could not be strictly followed in this paper. The definition of l_{tp} as the sum of shear-induced mixing length, l_{si}, and bubble-induced mixing length, l_b, used by Kataoka & Serizawa (1995a) and Kataoka & Serizawa (1995b) for analysis of bubbly flows with high Reynolds numbers is found to be inappropriate for here considered very slow bubble-driven liquid flows. In relation to this, it was reasonable to neglect l_{si} and assume $l_{tp} = l_b = \alpha_g d_b/3$.

The approaches used to evaluate ν_l^{eff} in two-equation models ($k-\varepsilon$ and algebraic stress models) can be classified into the following three groups:

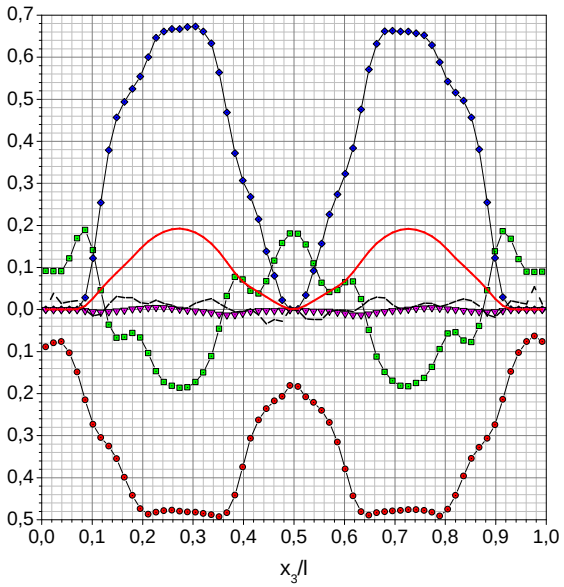

(a) scenario 8BM6

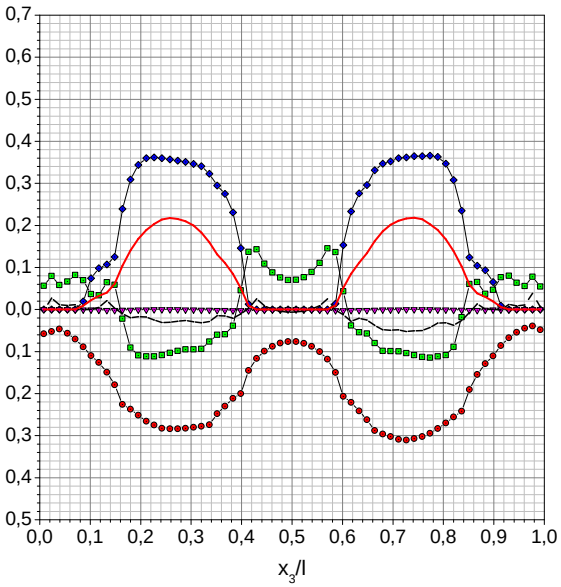

(b) scenario 8BM4

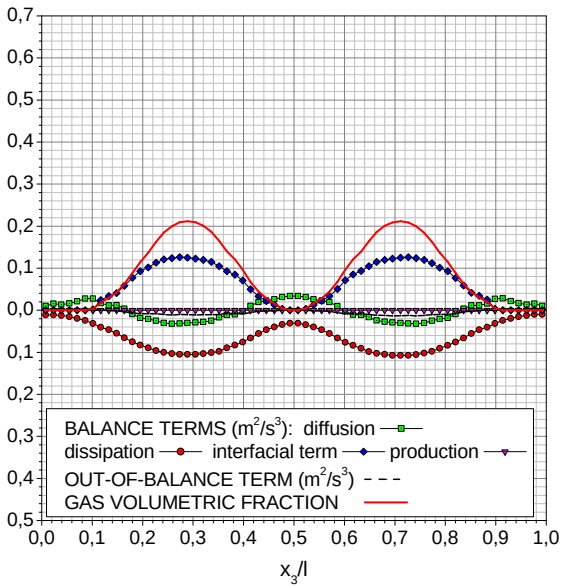

(c) scenario 8BM2

Figure 3: Budget of balance equation for turbulence kinetic energy of liquid phase (see equation 12) in bubbly flows with different viscosity. Notations given in c) apply to the whole Figure.

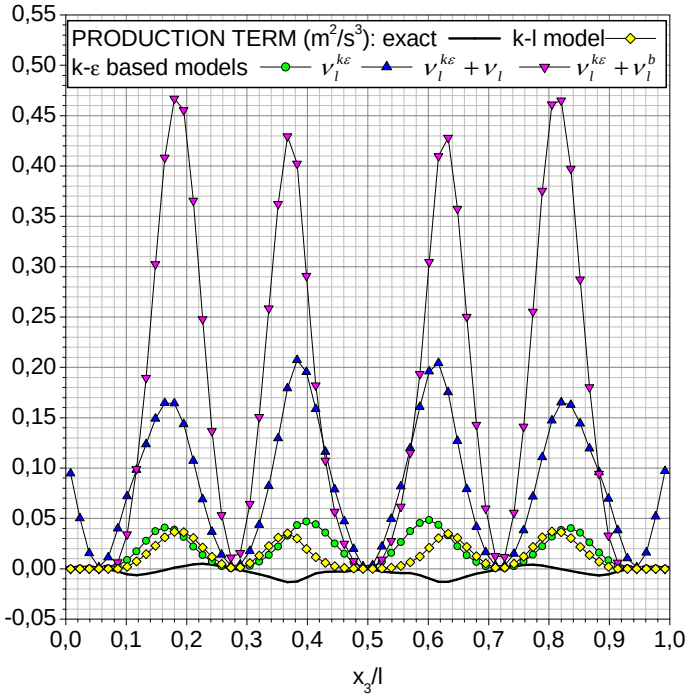

Figure 4: Performance of closure assumptions for production term in the case of bubbly flow scenario 8BM6.

- Only the eddy viscosity evaluated by two-phase $k-\varepsilon$ model, $\nu_l^{k\varepsilon}$, is considered (Boisson & Malin, 1996), (Grienberger & Hofmann, 1992), (Svendsen *et al.* , 1992), (Troshko & Hassan, 2001), (Politano *et al.* , 2003), (Morel, 1997), (Deen *et al.* , 2000), (Sheng & Irons, 1993), (Spicka *et al.* , 2001), (Hill *et al.* , 1995), (Mudde & Akker, 2001), (Oey *et al.* , 2003):

$$\nu_l^{\text{eff}} = \underbrace{C_\mu k_l^2/|\varepsilon_l|}_{\nu_l^{k\varepsilon}} \tag{15}$$

- Beside $\nu_l^{k\varepsilon}$ the molecular viscosity of the liquid phase, ν_l, is accounted for (Olmos *et al.* , 2003), (Pfleger & Becker, 2001):

$$\nu_l^{\text{eff}} = \underbrace{C_\mu k_l^2/|\varepsilon_l|}_{\nu_l^{k\varepsilon}} + \nu_l \tag{16}$$

- In addition to $\nu_l^{k\varepsilon}$ the bubble-induced eddy viscosity, ν_l^b, evaluated by model of Sato *et al.* (1981) is taken into consideration (Lahey & Drew, 1999):

$$\nu_l^{\text{eff}} = \underbrace{C_\mu k_l^2/|\varepsilon_l|}_{\nu_l^{k\varepsilon}} + \underbrace{0.6\alpha_g d_b|\overline{\overline{\mathbf{u}}}_r|}_{\nu_l^b}\,. \tag{17}$$

The following notation is used in the aforementioned relations: ε_l represents magnitude of the dissipation rate, $\overline{\overline{\mathbf{u}}}_r$ stands for the mean relative velocity between the phases and the coefficient $C_\mu = 0.09$.

The assessment of presented closure assumptions for production term is illustrated in Figure 4 for the bubbly flow scenario 8BM6 [2]. Figure 4 shows an extremely poor modelling of the production term - first, none of the applied closure assumptions was able to predict negative values of the production term evaluated by its basic mathematical formulation; second, absolute magnitudes of the production term are

[2]Results for bubbly flow scenarios 8BM4 and 8BM2 show approximatively the same relationship between the exact and modelled production term as observed in the case 8BM6 and are for that reason here not presented.

overestimated. However, while the overestimation is in the case of $k-l$ model and $k-\varepsilon$ where $\nu_l^{\text{eff}} = \nu_l^{k\varepsilon}$ moderate, it is strong for the case where $\nu_l^{\text{eff}} = \nu_l^{k\varepsilon} + \nu_l$ and drastic when bubble-induced eddy viscosity is accounted for ($\nu_l^{\text{eff}} = \nu_l^{k\varepsilon} + \nu_l^b$).

5.2 Redistribution of Liquid Turbulence Kinetic Energy

Like in single-phase flows the diffusion transport of liquid turbulence kinetic energy involves three contributions: pressure correlation, triple correlation and molecular diffusion (the first, the second and the third term on the r.h.s. of equation 12, respectively). The evaluation of corresponding diffusion subterms on the basis of their basic mathematical formulations given by equation 12 revealed a dramatic effect of the liquid viscosity on the role of mechanisms that govern the diffusion transport of the liquid turbulence kinetic energy. For instance, in the low viscosity case 8BM6 the transport of liquid turbulence energy from the domains with high gas volumetric fractions is mainly performed by pressure correlation and, at a lower extent, by triple correlation, while the contribution of the molecular diffusion is almost negligible. However, in domains with low gas volumetric fractions and in single-phase regions the relation between the different diffusion subterms significantly changes - the molecular diffusion gains on importance, while the triple correlation plays a minor role. The pressure correlation, however, represents a significant form of the diffusion transport over the whole domain. The increase of the liquid viscosity by factor of 3.162 (scenario 8BM4) affects the diffusion mechanisms appreciably - the transport by velocity fluctuations is completely dampened, while the contributions of the molecular diffusion and the pressure correlation are approximatively equal. The further increase of the liquid phase viscosity (scenario 8BM2) additionally suppresses the turbulent transport of liquid turbulence kinetic energy. Although the contribution of the pressure correlation in this case is lower than the one of the molecular diffusion, it is remarkable that even in such a very viscous liquid flow, the diffusion of liquid turbulence energy resulting from the correlation of pressure and velocity fluctuations is not to neglect.

The observed different intensity of the diffusive transport due to the fluctuating liquid flow makes questionable the validity of closure assumptions commonly used for the diffusion term. Current modelling of the diffusion in bubbly flows is, namely, based on closure relations well-established for single-phase forced flows, where the redistribution due to pressure fluctuations is of minor importance. In relation to this, the pressure correlation is grouped with the triple correlation and the sum is further modelled as a gradient-like process. Consequently, the total diffusion flux of k_l is expressed as:

$$\text{Diff}(k_l) = \nabla \cdot [\alpha_l \nu_l^{\text{Diff}} \nabla k_l], \tag{18}$$

where ν_l^{Diff} represents the diffusion coefficient. In one-equation models the diffusion coefficient is given by ((Kataoka & Serizawa, 1995a) and (Kataoka & Serizawa, 1995b)):

$$\nu_l^{\text{Diff}} = \underbrace{0.5\nu_l + \beta_2 l_{tp}\sqrt{k_l}}_{\nu_l^{kl}}, \tag{19}$$

where the coefficient $\beta_2 = 0.38$, while in two-equation models ν_l^{Diff} is evaluated in the analogous way as the effective eddy viscosity, ν_l^{eff}, i.e.:

- $\nu_l^{\text{Diff}} = \nu_l^{k\varepsilon}$ (Troshko & Hassan, 2001), (Politano *et al.* , 2003), (Morel, 1997), (Deen *et al.* , 2000), (Sheng & Irons, 1993);
- $\nu_l^{\text{Diff}} = \nu_l^{k\varepsilon} + \nu_l$ (Boisson & Malin, 1996), (Grienberger & Hofmann, 1992), (Svendsen *et al.* , 1992), (Spicka *et al.* , 2001), (Olmos *et al.* , 2003), (Hill *et al.* , 1995), (Mudde & Akker, 2001), (Oey *et al.* , 2003), (Pfleger & Becker, 2001);
- $\nu_l^{\text{Diff}} = \nu_l^{k\varepsilon} + \nu_l^b$ (Lahey & Drew, 1999).

The performance of the above presented closure assumptions for the diffusion term is illustrated in Figure 5 for the bubbly flow scenarios 8BM2 and 8BM6. It can be seen that closure assumptions used

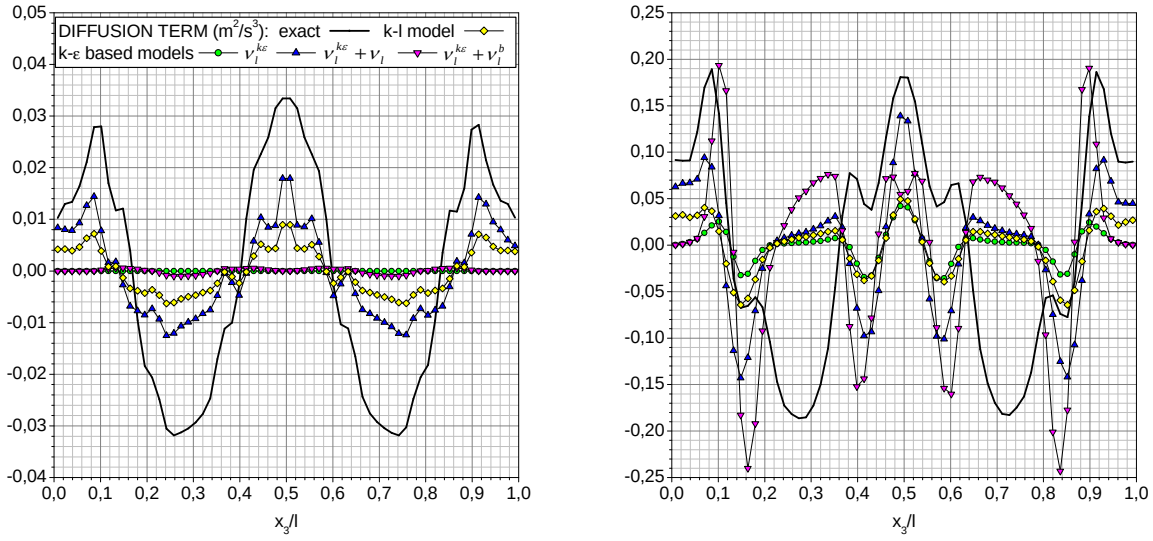

(a) scenario 8BM2 (b) scenario 8BM6

Figure 5: Performance of closure assumptions for the diffusion term in k_l equation for bubbly flows with different viscosity. Notations given in a) apply to the whole Figure.

in $k-l$ and in $k-\varepsilon$ models where $\nu_l^{\mathrm{Diff}} = \nu_l^{k\varepsilon} + \nu_l$ in the case 8BM2 underestimate the magnitudes of the diffusion term, but correctly predict the shape of the diffusion profile over the whole channel width. Such a situation is to be expected since in this, the most viscous, case significant contribution to the exact diffusion term is made by the molecular diffusion that is in these approaches included through ν_l. On the other side, closures where the liquid viscosity is not taken into account totally failed estimating approximatively zero values of the diffusion term.

While the presented results for the scenario 8BM2 give a hope that acceptable modelling of the diffusion term could be achieved establishing a proper closure for the diffusion coefficient, ν_l^{Diff}, the predictions of the diffusion term for the bubbly flow case with the lowest liquid viscosity (scenario 8BM6) clearly indicate that the whole concept of currently used engineering formulations for the diffusion transport of liquid turbulence kinetic energy in bubbly flows is inappropriate. In Figure 5b it can, namely, be seen that dramatic disagreement between the modelled and exact diffusion terms occurs in two-phase regions of the channel - not only the magnitudes of the diffusion term are incorrectly predicted, but, also, its sign. The attempt to include the two-phase effects in the diffusion coefficient through the bubble-induced eddy viscosity, ν_l^b, resulted even in higher discrepancies.

5.3 Viscous Dissipation of Liquid Turbulence Kinetic Energy

While the production and diffusion of liquid turbulence kinetic energy are in all the considered models expressed in the form of closure assumptions, the dissipation term in $k-\varepsilon$ and algebraic stress models is evaluated by a separate transport equation. In this context, discussions concerning the dissipation term are restricted on closure assumptions used in the one-equation $k-l$ model. Therefore, Kataoka & Serizawa (1995a) and Kataoka & Serizawa (1995b) proposed the following closure assumption for the dissipation rate:

$$\varepsilon_l = \gamma_1 \alpha_l k_l^{3/2} / l_{tp}, \tag{20}$$

where the coefficient $\gamma_1 = 0.18$.

Results obtained using the above definition of the dissipation term are presented in Figure 6. Since two-phase mixing length, l_{tp}, as defined in this work involves only the bubble-induced contribution, the

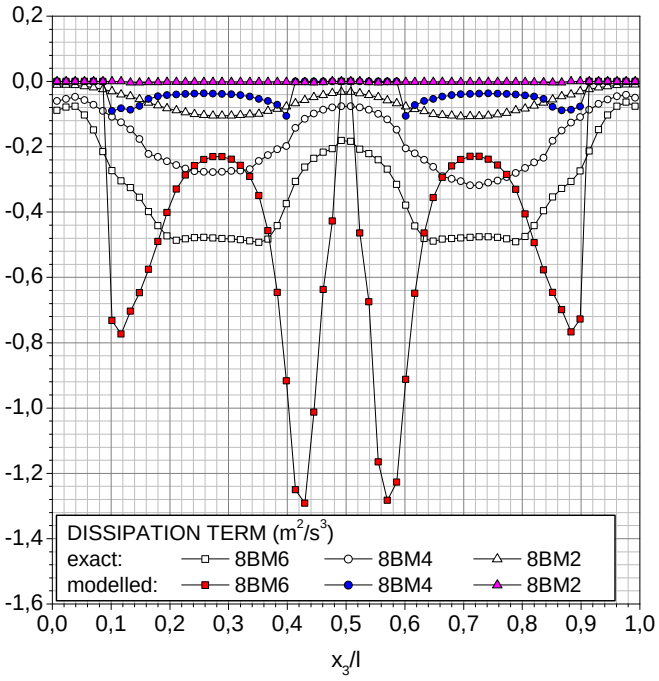

Figure 6: Predictions of dissipation term by $k-l$ models for bubbly flows with different viscosity.

dissipation rate in channel regions permanently occupied by the liquid phase could not be computed. The comparison of the modelled dissipation term with the exact one shows poor performance of the expression 20 for all the considered bubbly flow scenarios.

5.4 Interfacial Generation of Turbulence Kinetic Energy

The interfacial terms as given in equation 12 can, after some simple mathematical manipulations, be expressed in the following form (Troshko & Hassan, 2001):

$$\Upsilon_l = \frac{1}{\varrho_l}\overline{\mathbf{u}'_{li}\underbrace{\left[-\left(p_{li}-\overline{\overline{p}}_{li}\right)\mathbf{I}+\tau_{li}\right]}_{\mathbf{M}_l}\nabla\Phi_l} - \frac{1}{\varrho_l}\left[\left(\overline{\overline{p}}_{li}-\overline{\overline{p}}_l\right)\mathbf{I}+\overline{\overline{\tau}}_l\right] : \overline{\mathbf{u}'_{li}\nabla\Phi_l}, \tag{21}$$

where the unit tensor is denoted by $\mathbf{I}$, the gradient of the liquid phase indicator function is given as $\nabla\Phi_l = \mathbf{n}_l a_i$ and the average interfacial pressure of the liquid phase is defined as $\overline{\overline{p}}_{li} = \overline{p_{li}a_i}/\overline{a_i}$ (Kataoka & Serizawa, 1989), while $\mathbf{M}_l$ represents the instantaneous interfacial force density (Drew, 1983).

Evaluations performed using DNS data for here considered bubbly flows have revealed that the contribution of the first term in expression 21 to the total interfacial generation of liquid turbulence energy is absolutely dominant comparing to the contribution of the second term. Assuming that the aforementioned conclusion about the negligible contribution of the correlation between the velocity fluctuations and the interface dynamics may, also, be extended to the gas phase ($\overline{\mathbf{u}'_g\nabla\Phi_g} \sim 0$) the interfacial generation of the turbulence kinetic energy in two-phase mixture, Υ_{tp}, can be given as:

$$\varrho_{tp}\Upsilon_{tp} = \varrho_l\Upsilon_l + \varrho_g\Upsilon_g = \sum_{k=l,g}\overline{\mathbf{u}'_{ki}\mathbf{M}_k}, \tag{22}$$

where Υ_g represents the interfacial generation of gas turbulence kinetic energy and the subscripts k and tp indicate the phase (liquid or gas) and the two-phase mixture, respectively. Having in mind the definition

Model	Contributions to interfacial terms	
	Drag	Non-drag
M1 (Morel, 1997)	$\underbrace{\frac{3}{4}C_d\varrho_l\alpha_g\lvert\overline{\overline{\mathbf{u}}}_r\rvert^3/d_b}_{W^d}$	$\mathbf{M}_{am}\cdot\overline{\overline{\mathbf{u}}}_r$
M2 (Boisson & Malin, 1996)	$0.05\alpha_l W^d$	None
M3 (Olmos *et al.* , 2003)	$0.75W^d$	None
M4 (Pfleger & Becker, 2001)	$1.44W^d$	None
M5 (Kataoka & Serizawa, 1995a)	$0.075f_w\frac{3}{4}C_d\varrho_l\alpha_g u_t^3/d_b$	$\alpha_g\varrho_l k_l^{2/3}/d_b$
M6 (Lahey & Drew, 1999)	$0.25\alpha_l\alpha_g(1+C_d^{4/3})\lvert\overline{\overline{\mathbf{u}}}_r\rvert^3/d_b$	None
M7 (Sheng & Irons, 1993)	$0.6\frac{3}{4}\varrho_l C_d\frac{\alpha_g}{d_b}\lvert\overline{\overline{\mathbf{u}}}_r\rvert k_l$	$2.53\alpha_g\alpha_l\Pi_l$
M8 (Hill *et al.* , 1995)	$\frac{3}{4}\frac{C_d}{d_b}\lvert\overline{\overline{\mathbf{u}}}_r\rvert\left(2\alpha_g\varrho_l(C_t-1)k_l-\frac{\nu_l^{k\varepsilon}}{\alpha_l\alpha_g}\overline{\overline{\mathbf{u}}}_r\cdot\nabla\alpha_g\right)$	None

Table 2: List of currently used engineering formulations for interfacial turbulence transfer in bubbly flows.

of interfacial velocity fluctuation, $\mathbf{u}_{ki}^{'}=\mathbf{u}_{ki}-\overline{\overline{\mathbf{u}}}_k$, the equality of phase interface velocities in the absence of phase change, $\mathbf{u}_{li}=\mathbf{u}_{gi}$, and validity of the principle of action and reaction on the phase interface, $\mathbf{M}_l=-\mathbf{M}_g$, the expression 22 can be given in the following form:

$$\Upsilon_l=\frac{1}{\varrho_l}\overline{\mathbf{M}_l}(\overline{\overline{\mathbf{u}}}_l-\overline{\overline{\mathbf{u}}}_g)-\frac{\varrho_g}{\varrho_l}\Upsilon_g. \tag{23}$$

The benefit of the relation 23 is indispensable for engineering considerations of the liquid turbulence in bubbly flows. As in typical bubbly gas-liquid flows, namely, the ratio of phase densities, ϱ_g/ϱ_l, is very low, it is reasonable to neglect the second term in expression 23 and express the interfacial generation of the liquid turbulence kinetic energy as the rate at which the work is performed by interfacial forces in relative motion of bubbles. However, since bubbly flows considered here are associated with the high density ratio ($\varrho_g/\varrho_l=0.5$), the second term on the right-hand-side of equation 23 has to be taken into account. In this context, the performance of closure assumptions for interfacial turbulence energy transfer is tested against the following sum:

$$\Upsilon=\Upsilon_l+\frac{\varrho_g}{\varrho_l}\Upsilon_g, \tag{24}$$

where Υ_g is evaluated replacing the subscript l in expression for Υ_l (see equation 12) by the subscript g.

Literature overview of closure assumptions for effects of bubble interfaces on the liquid phase turbulence has shown that the aforementioned concept is followed - the interfacial term is in various ways related to the rate of work performed by interfacial forces. An inspection of the reported formulations further revealed that in development of closure assumptions for Υ bubbly flows are, generally, considered to be drag dominated. Therefore, in Table 2 it can be seen that the drag contribution, Υ^d, is included in all the models, while in models M2, M3, M4, M6 and M8 it is even considered to be the only one. In the model M1 Υ^d is equal to the total power of drag force, $\Upsilon^d=W^d$, in models M2, M3 and M4 Υ^d is equal to a portion, C_b, of the total power of the drag force, $\Upsilon^d=C_bW^d$, while in the models M6, M7 and M8 the power of the drag force is not explicitly contained in Υ^d. Except for the model M5, where the evaluation of the drag is based on terminal velocity $u_t=1.414\left[\sigma|\mathbf{g}|(\varrho_l-\varrho_g)/\varrho_l^2\right]^{0.25}$, in all other models the mean relative velocity between phases, $|\overline{\overline{\mathbf{u}}_r}|$, is used. The drag coefficient in models M1, M5 and M8 is evaluated from the 'standard' relation:

$$C_d=\frac{2}{3}\sqrt{E\ddot{o}_b}\underbrace{\frac{1+17.67\alpha_l^{1.3}}{18.67\alpha_l^{1.5}}}_{f_\alpha}, \tag{25}$$

where $E\ddot{o}_b$ represents bubble Eötvös number and f_α takes into account multiple bubble effects. Since in models M6 and M7 the applied relation for C_d is not reported, in here performed computations the expression 25 is used. In the model M3 drag coefficient is determined as $C_d = \frac{2}{3}\sqrt{E\ddot{o}_b}(1-\langle\alpha_g\rangle)^p$, where p represents an integer dependent on the bubble diameter and gas superficial velocity (for conditions of bubbly flows considered here p takes the value of 0). In the model M4 $C_d = 0.44$, while in the model M2 $C_d = 20.68/Re_b^{0.643}$, where the bubble Reynolds number is defined by $Re_b = |\overline{\overline{\mathbf{u}}}_r|d_b/\nu_l$. Van Driest's function, f_w, used in the model M5 is formulated in the same way as in single-phase flows. For the definition of the coefficient C_t in the model M8 see the corresponding reference.

The non-drag contributions to the interfacial terms, Υ^{nd}, are taken into account only by a few authors. Therefore, in the model M1 the work of the added mass force, $\mathbf{M}_{am} = C_{am}\frac{1+2\alpha_g}{1-\alpha_g}\alpha_g\varrho_l\left(\frac{D_g\overline{\overline{\mathbf{u}}}_g}{Dt} - \frac{D_l\overline{\overline{\mathbf{u}}}_l}{Dt}\right)$, is included ($C_{am}$ is the added mass coefficient), in the model M5 the term that accounts for absorption of liquid turbulence by bubbles is considered, while in the model M7 Υ^{nd} is related to the liquid turbulence production by mean shear, Π_l.

The performance of all the presented closure assumptions is first tested for the bubbly flow scenario 8BM6 (see Figure 7). The analyses of obtained results revealed the following:

- All the non-drag contributions are an order of magnitude lower than the corresponding drag ones.
- Models M2, M5, M7 and M8 totally fail predicting almost zero magnitudes of interfacial terms.
- Models M3, M4 and M6 underestimate the magnitudes of interfacial terms.
- Model M1 gives acceptable discrepancies and seems to be the promising approach in modelling of interfacial terms.

The encouraging performance of the model M1 in the simulation scenario 8BM6 has, however, not been obtained when bubbly flows 8BM4 and 8BM2 were considered - interfacial terms have been strongly underestimated in both cases. Taking into account significantly different flow conditions in scenarios 8BM2 and 8BM4 this situation is suspected to be assigned to the inappropriate formulation of the drag coefficient. The correlation for the drag coefficient given by expression 25 is, namely, developed for the most often used suspension of air bubbles in water - its applicability to bubbly flows 8BM4 and especially 8BM2 is, therefore, seriously limited due to the increased liquid viscosity. In relation to this, it is supposed that the better performance of the model M1 can be achieved by use of drag coefficient correlations reported by Tomiyama (1998), that have experimentally been verified within a wide range of fluid properties (bubble Eötvös number $E\ddot{o}_b = 10^{-2} - 10^3$, Morton number, $M = 10^{-14} - 10^7$ and bubble Reynolds number, $Re_b = 10^{-3} - 10^5$). For a pure gas-liquid system considered in this paper the drag coefficient relation is formulated by:

$$C_d = max\left[min\left(\frac{16}{Re_b}, (1+0.15Re_b^{0.687})\right), \frac{8}{3}\frac{E\ddot{o}_b}{E\ddot{o}_b+4}\right]. \tag{26}$$

The evaluation of interfacial terms as defined by the model M1, but with the drag coefficient defined by 26 instead of 25, has confirmed the importance of the proper choice of the drag coefficient formulation. Therefore, as it can be seen in Figure 8, despite the discrepancies between the modelled and the exact interfacial term profiles, the modelling concept proposed by Morel (1997) (model M1) may be judged as correct. Further, when one takes into account that in Figure 8 results computed by a semi-empirical engineering approach are drawn versus the ones evaluated on the basis of rigid mathematical formulations for an extremely wide range of bubbly flow parameters, it may be stated that modelling of the interfacial turbulence effects by the model M1 is acceptable.

The results presented in this and in the previous section have revealed that in dilute bubble-driven liquid flows the rate of the work done by bubbles on the continuous phase is, on overall level, balanced by the viscous dissipation term (the magnitude of the production term is negligible and the diffusion term

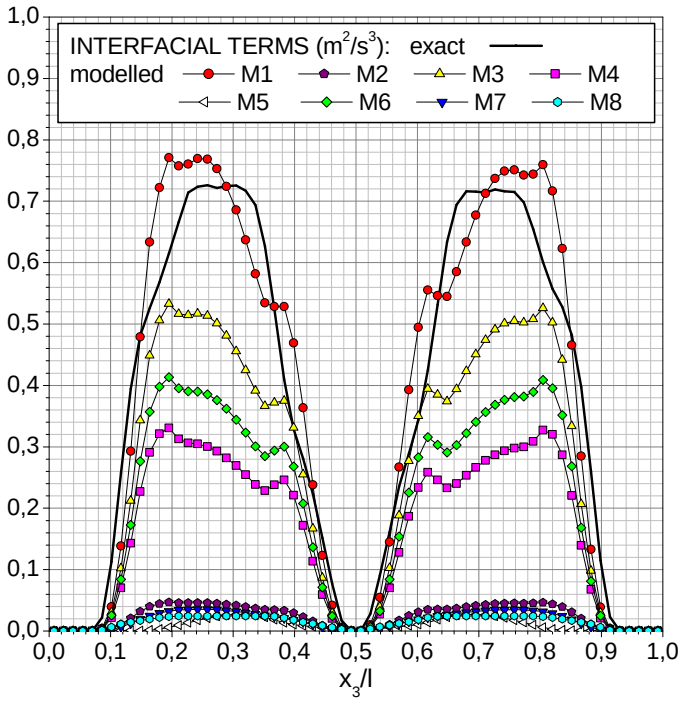

Figure 7: Performance of closure assumptions for interfacial turbulence transfer in the case of bubbly flow scenario 8BM6.

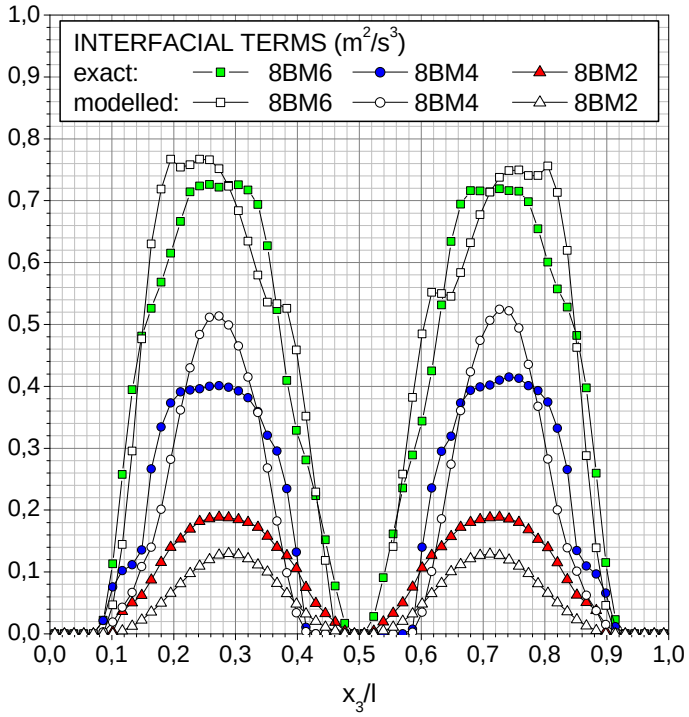

Figure 8: Predictions of interfacial turbulence transfer by model M1 using the drag coefficient relation 26.

has no net contribution). Therefore, in a steady drag dominated bubbly flow the overall dissipation rate, $\langle \varepsilon_l \rangle$, can be expressed using an appropriate empirical correlation for the power of the drag force. This fact is here used to check whether the computational grid 64^3 imposed on flow domain is sufficiently fine to resolve the smallest vortices. In relation to the aforementioned, the well-known definition for Kolmogorov length scale $\eta = \nu_l^{3/4} |\langle \varepsilon_l \rangle|^{-1/4}$, takes the following form:

$$\eta = d_b \left[\frac{4}{3} \frac{1}{C_d \varrho_l \langle \alpha_g \rangle} \right]^{\frac{1}{4}} Re_b^{-\frac{3}{4}}, \tag{27}$$

where the bubble Reynolds number is defined on the bases of overall phase relative velocity, $\langle \overline{\overline{u}}_r \rangle$. The values of Kolmogorov length scale evaluated using the drag coefficient correlation 26: $\eta^{8BM6} = 2.4788\Delta x$, $\eta^{8BM4} = 7.4935\Delta x$ and $\eta^{8BM2} = 22.1151\Delta x$ demonstrate that the requirement $\eta > 2\Delta x$ is satisfied in all the simulation cases.

6 CONCLUSIONS

This paper reports investigations of liquid phase turbulence in slow dilute bubbly flows. Investigations are based on statistical analysis of liquid velocity fluctuations, where the liquid turbulence kinetic energy is considered as the fundamental turbulence quantity. The main goal of the performed analysis was to improve understanding of mechanisms in which bubbles alter generation, redistribution and dissipation of turbulence kinetic energy in the liquid phase. Second issue concerns assessment of closure assumptions commonly used in engineering liquid turbulence models.

Input data for the liquid turbulence analysis are provided by direct numerical simulations of bubbly flows. In total three numerical runs were performed, where the rise of bubble swarms consisting of 8 bubbles within cubic channel with two lateral walls is simulated. The influence of bubble shape and bubble rise velocity on characteristics of generated liquid flow is analyzed specifying different liquid viscosities.

It has been found that the increase of the liquid viscosity causes a drastic decrease of the liquid turbulence kinetic energy. Three flow parameters have been identified as reasons for such a behaviour of the liquid turbulence energy: decrease of the bubble rise velocity between the phases, the change of bubble shape from ellipsoidal to spherical (reflected through the decrease of added mass) and the suppression of vortical structures in bubble wakes.

An attempt to elucidate physical mechanisms in which bubbles alter the liquid turbulence is made by evaluation of balance terms in the basic equation for the liquid turbulence kinetic energy. The main conclusions from this analysis are as follows. The transfer of kinetic energy between the mean and fluctuating liquid flow (so-called production term) is negligible. The generation of liquid turbulence kinetic energy is, therefore, continuously maintained only through the work of fluctuating liquid stress upon the moving bubble interfaces. Since this term has a local character determined by the distribution of bubbles, the local non-equilibrium between the turbulence generation and turbulence dissipation gives importance to the diffusion term. A detailed analysis of the diffusion subterms has shown that the molecular transport process plays an important role and may, therefore, not be neglected in slow bubble-driven liquid flows. An especially important form of the diffusive transport in all the considered bubbly flows turned out to be correlation including pressure fluctuations.

DNS based evaluations of balance terms in the basic equation for liquid turbulence kinetic energy are, further, used to assess performance of corresponding closure assumptions applied in engineering models for the liquid phase turbulence. The performed analysis have revealed the following. Currently used closure assumptions failed to realistically predict both, the production term and the diffusion term - while the production term is strongly overestimated, the diffusion transport of liquid turbulence kinetic energy is strongly underestimated by all closure assumptions. When the performance of closure assumptions for the interfacial term is concerned, encouraging results are obtained. Therefore, although majority of the

available closure assumptions resulted in the strong underestimation of this term, predictions made by the model of Morel (1997) are quite acceptable. An inspection of the results obtained by this modelling approach indicated that the interfacial term can be formulated very simply - as the rate at which the work of the drag force is performed. It is, however, emphasized, that a great caution has to be paid when the closure relation for the drag coefficient is specified. According to the analysis performed here, the use of drag coefficient relations proposed by Tomiyama (1998) is suggested.

REFERENCES

Boisson, N., & Malin, M. R. 1996. Numerical prediction of two-phase flow in bubble columns. *International Journal for Numerical Methods in Fluids*, **23**, 1289–1310.

Bunner, B., & Tryggvason, G. 2003. Effect of bubble deformation on the properties of bubbly flows. *Journal of Fluid Mechanics*, **495**, 77–118.

Clift, R., Grace, J. R., & Weber, M. F. 1978. *Bubbles, drops and particles*. New York: Academic Press.

Deen, N. G., Solberg, T., & Hjertager, B. H. 2000. Numerical simulation of the gas-liquid flow in a square cross-sectioned bubble column. *In: Proc. of* 14^{th} *Conference of Chemical and Process Engineering*.

Drew, D. A. 1983. Mathematical modelling of two-phase flow. *Ann. Rev. Fluid Mech*, **15**, 261–291.

Grienberger, J., & Hofmann, H. 1992. Investigation and modelling of bubble columns. *Chemical Engineering Science*, **47**, 2215–2220.

Hill, D. P., Wang, D. M., Gosman, A. D., & Issa, R. I. 1995. Numerical prediction of two-phase bubbly flow in a pipe. *In: Proc. of the* 2^{nd} *International Conference on Multiphase Flow*.

Kataoka, I., & Serizawa, A. 1989. Basic equations of turbulence in gas-liquid two-phase flow. *International Journal of Multiphase Flow*, **15**, 843–855.

Kataoka, I., & Serizawa, A. 1995a. Modelling and prediction of turbulence in bubbly two-phase flow. *In: Proc. of* 2^{nd} *International Conference on Multiphase Flow*.

Kataoka, I., & Serizawa, A. 1995b. Modelling and prediction of turbulence in bubbly two-phase flow. *In: Proc. of Two-phase Flow Modelling and Experimentation.*

Lahey, R. T., & Drew, D. 1999. An analysis of two-phase flow and heat transfer using a multidimensional, multi-field, two-fluid computational fluid dynamics (CFD) model. *In: Japan/US Seminar on Two-Phase Flow Dynamics*.

Morel, C. 1997. Turbulence modelling and first numerical simulations in turbulent two-phase flows. *In: Proc. of the* 11^{th} *Symposium on Turbulent Shear Flows*.

Mudde, R. F., & Akker, H. E. A. Van Den. 2001. 2D and 3D simulations of an internal airlift loop reactor on the basis of a two-fluid model. *Chemical Engineering Science*, **56**, 6351–6358.

Oey, R. S., Mudde, R. F., & Akker, H. E. A. Van Den. 2003. Sensitivity study on Interfacial closure laws in two-fluid bubbly flow simulations. *AIChE Journal*, **49**, 1621–1636.

Olmos, E., Gentric, C., & Midoux, N. 2003. Numerical description of flow regime transitions in bubble column reactors by a multiple gas phase model. *Chemical Engineering Science*, **58**, 2113–2121.

Pfleger, D., & Becker, S. 2001. Modelling and simulation of the dynamic flow behaviour in a bubble column. *Chemical Engineering Science*, **56**, 1737–1747.

Politano, M. S., Carrica, P. M., & Converti, J. 2003. A model for turbulent polydisperse two-phase flow in vertical channels. *International Journal of Multiphase Flow*, **29**, 1153–1182.

Sabisch, W., Wörner, M., Grötzbach, G., & Cacuci, D. G. 2001. 3D volume-of-fluid simulation of a wobbling bubble in a gas-liquid system of low Morton number. *In: Proc. of 4th International Conference on Multiphase Flow*.

Sato, Y., Sadatomi, M., & Sekoguchi, K. 1981. Momentum and heat transfer in two-phase bubble flow - I. *Journal of Multiphase Flow*, **7**, 167–177.

Sheng, Y. Y., & Irons, G. A. 1993. Measurements and modelling of turbulence in the gas-liquid two-phase zone during gas injection. *Metallurgical Transactions B*, **24B**, 695–705.

Spicka, P., Dias, M. D., & Lopes, J. C. B. 2001. Gas-liquid flow in a 2D column: Comparison between experimental data and CFD modelling. *Chemical Engineering Science*, **56**, 6367–6383.

Svendsen, H. F., Jakobsen, H. A., & Torvik, R. 1992. Local flow structures in internal loop and bubble column reactors. *Chemical Engineering Science*, **47**, 3297–3304.

Tomiyama, A. 1998. Struggle with computational bubble dynamics. *In: Proc. of 3rd International Conference on Multiphase Flow*.

Troshko, A. A., & Hassan, Y. A. 2001. A two-equation turbulence model of turbulent bubbly flows. *International Journal of Multiphase Flow*, **27**, 1965–2000.

Wijngaarden, L. Van. 1998. On pseudo turbulence. *Theoretical and Computational Fluid Dynamics*, **10**, 449–458.